JOURNAL OF MODERN OPTICS
2003, VOL. 50, NO. 15–17, 2691–2704

Taylor & Francis
Taylor & Francis Group

The geometric structure and optical response of gaseous endohedral magnesium–fullerenes

M. AICHINGER‡, S. A. CHIN†, E. KROTSCHECK‡ and H. A. SCHUESSLER†

†Department of Physics, Texas A&M University, College Station, TX 77843, USA

‡Institut für Theoretische Physik, Johannes Kepler Universität, A 4040 Linz, Austria

(*Received 15 April 2003*)

Abstract. Using density functional theory, a jellium model for the C_{60} molecule and a pseudopotential for the magnesium ion, we determined the energetics of the magnesium endohedral complex as a function of the magnesium ion's displacement from the fullerene's centre. The resulting Kohn–Sham equation is solved in cylindrical coordinates. Our calculation shows that the magnesium ion will reside in a very shallow energy minimium about ≈ 1 Å off centre. By computing the photoabsorption cross-section, or the imaginary part of the dynamic polarizability, we can correlate the displacement of the magnesium ion with a peak shift in the photoabsorption cross-section. This suggests that the location of the magnesium ion inside C_{60} can be determined experimentally by observing the optical response of the endohedral complex.

1. Introduction

Endohedral fullerenes are compounds with unique structure [1, 2]. Carbon atoms in these compounds form a cage enclosing an atom, insulating it from the environment and at the same time modifying its properties. Figure 1 depicts endohedral and exohedral metalofullerene complexes and lists some of their basic properties. The endohedral system, which is the subject of this paper, has the metal atom inside the carbon cage. In the exohedral system, the metal atom resides on the cage itself. The chemical and optical properties of the fullerene are also altered by the presence of the atom. This remarkable mutual interaction is of great fundamental interest and endohedral fullerenes have been elevated to the status of super atoms [3]. It is believed that endohedral fullerene compounds, after having been well studied, will provide numerous applications ranging from superconducting materials to biological markers in magnetic resonance imaging [1]. The interaction of these natural nanostructures with optical radiation and their long time storage in an ion trap [4] opens up novel spectroscopies of large molecules floating in free space, including the possibility of resonance excitation transfer from an endohedral to an exohedral complex. In particular the optical spectrum of gaseous endohedral fullerenes promises narrow and distinct transitions. In the past, the magnesium ion has been a test case for many questions concerning the interaction of light with materials [5, 6] due to its simple structure and intense resonance lines. Therefore, it was decided to use magnesium as an initial probe for

Journal of Modern Optics ISSN 0950–0340 print/ISSN 1362–3044 online
http://www.tandf.co.uk/journals
DOI: 10.1080/0950034032000120731

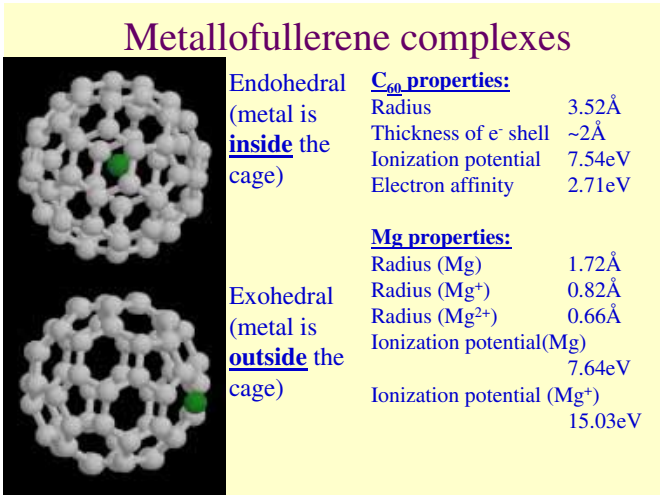

Figure 1. Compilation of basic properties of endohedral and exohedral metallofullerene complexes.

the study of endohedral fullerene interactions [4]. Large clouds of magnesium fullerene complexes have been trapped for long periods of time (many hours) so that all excitations have had time to relax to their lowest states. Both pure endohedral and pure exohedral gaseous magnesium fullerene complexes have been produced by changing the collisional production conditions [7]. This continuing work is motivated by several considerations. First, there is the question of determining the location of the magnesium ion inside the fullerene. Second, possible quantum electrodynamics (QED) effects need to be verified in a novel region, where the wavelength is much larger than the fullerene cavity. Third, the results of photo-ionization and photo-fragmentation experiments [8–10] must be extended by studying optical excitations between well-defined internal states, such as low initial and highly excited final states.

Current optical experiments have the potential to observe the location of the entrapped atom. This location depends on the particular endohedral atom studied, and ranges from being fixed at the centre to significantly off centre [11–14]. The theoretical determination of this geometric structure involves the minimization of the total energy of a many-electron system. Density functional (DF) theory [15, 16], specifically in the local density approximation (LDA) has been widely applied (with well-known shortcomings) to large non-uniform electronic systems. For some molecules and especially clusters [17] the spherical symmetric DFT has given results in good agreement with experimental data. In this theoretical work, we have implemented a newly developed response algorithm [18] for solving the Kohn–Sham equation in non-spherical geometry, allowing us to directly determine the energetics of an endohedral complex as a function of the off-centre displacement of the enclosed ion.

In an early restricted Hartree–Fock calculation of Cioslowski and Fleischmann [12], the second derivative of the total energy with respect to enclosed ion's displacement at the origin has been found to be small but negative for F^-, Na^+ and Mg^{++}, suggesting that for these ions, the fullerene centre is an unstable

equilibrium point. A later calculation by Schmid *et al*. [14] comfirmed that Na^+ is indeed off-centre, for about 0.6 to 0.7 Å. In this work, we study the structure and optical response of the endohedral complex $Mg@C_{60}^+$, $Mg@C_{60}$ and $Mg@C_{60}^-$. Since the caged ion's off-centre displacement is expected to be small, it should not be sensitive to the discrete ionic character of the C_{60} shell far away. Thus it is adequate for our purpose to use a jellium model of C_{60} [19] in our DFT calculation. By solving for the full spectrum of the axial symmetric Kohn–Sham equation in 2D, we not only can determine the entrapped atom's equilibrium location, but also its effect on the complex's photoabsorption cross-section. One key finding of our work is that a discrete absorption peak will shift toward higher energy as the entrapped atom moves off centre, suggesting the possibility of experimentally determing the entrapped atom's location by monitoring the endohedral complex's optical response.

In the next two sections, we briefly summarize essential elements of DFT and our magnesium pseudopotential. In section 4, we describe our axial symmetric calculation. In section 5 we discuss our results on the magnesium ion's delocalization, the conspicuous energy shift of the 3s state as a function of the ion's position, and the corrresponding shift of a resonance peak in the photoabsorption cross-section. Conclusions are presented in section 6.

2. Density functional calculation

Central to the execution of density functional theory is the solution of the Kohn–Sham (KS) equation for a set of single-particle wavefunctions $\psi_{\mathbf{i}}(\mathbf{r})$ characterized by a set of quantum numbers $\mathbf{i}$:

$$-\frac{\hbar^2}{2m}\nabla^2\psi_{\mathbf{i}}(\mathbf{r}) + V_{\mathrm{H}}[\rho](\mathbf{r})\psi_{\mathbf{i}}(\mathbf{r}) = \varepsilon_{\mathbf{i}}\psi_{\mathbf{i}}(\mathbf{r}). \tag{1}$$

The effective one-body ('Hartree') potential $V_{\mathrm{H}}(\mathbf{r})$, given by

$$V_{\mathrm{H}}(\mathbf{r}) = V_{\mathrm{ext}}(\mathbf{r}) + V_{\mathrm{C}}(\mathbf{r}) + V_{\mathrm{xc}}(\mathbf{r}) \tag{2}$$

describes both the influence of an external field (typically the positive ions) and many-body interactions. It depends implicitly on the density of the system: $V_{\mathrm{ext}}(\mathbf{r})$ is the external field, $V_{\mathrm{C}}(\mathbf{r})$ is the Coulomb potential

$$V_{\mathrm{C}}(\mathbf{r}) = \int \mathrm{d}^3r' \frac{e^2}{|\mathbf{r}-\mathbf{r}'|}[\rho(\mathbf{r}') - \rho_+(\mathbf{r}')], \tag{3}$$

and $V_{\mathrm{xc}}(\mathbf{r})$ is the 'exchange-correlation' correction. $\rho_+(\mathbf{r}')$ is the charge density of the positive background.

From the single-particle wave functions $\phi_{\mathbf{i}}(\mathbf{r})$ one constructs the physical one-body density

$$\rho(\mathbf{r}) = \sum_{\mathbf{i}} n(\mathbf{i})\left|\psi_{\mathbf{i}}(\mathbf{r})\right|^2; \tag{4}$$

the $n(\mathbf{i})$ are the occupation numbers of the single-particle states.

To describe the C_{60} molecule within a jellium model, we followed the work of Puska and Nieminen [19] and approximated the discrete ionic charges by a

uniform, positve spherical shell charge density

$$n_+(r) = \begin{cases} n_0, & \text{when } R - \dfrac{\Delta R}{2} \le r \le R + \dfrac{\Delta R}{2}, \\ 0, & \text{elsewhere.} \end{cases} \tag{5}$$

The thickness ΔR of the shell is determined by requiring charge neutrality of the *undoped neutral cluster* with 240 electrons. The positive background density was chosen, following [19] to correspond to an r_s value of 1.2. From this, the shell thickness comes out to be approximately 3 au. To correct for this simple approximation, we also adopted Puska and Nieminen's strategy of adding an additional potential $v_{ps}(r)$ inside the jellium density shell,

$$v_{ps}(r) = \begin{cases} -v_0, & \text{when } R - \dfrac{\Delta R}{2} \le r \le R + \dfrac{\Delta R}{2}, \\ 0, & \text{elsewhere,} \end{cases} \tag{6}$$

with $v_0 = -1.4$ Ryd. One refinement that we have implemented over [19] is that we have correctly 240 conduction electrons (instead of the closed shell value of 250). The last shell is then only partially filled; we achieve stability for this configuration by giving the electrons a small artificial temperature of 0.07 eV. We have verified that the results are insensitive to that 'temperature' down to 10^{-8} eV.

As noted by Puska and Nieminen, this jellium model gives a rather good description of the lowest four dipole-allowed optical transitions. Four strong absorption bands are observed with peaks at ≈3.0, 3.6, 4.7 and 5.7 eV for both solid C_{60} film and C_{60} in solution [20]. The four lowest dipole transitions in our jellium model are at 3.2, 3.7, 4.9 and 5.3 eV respectively.

The icosahedral symmetry of C_{60} can be included and treated as a perturbation [21]. However, as we will see, the state that is strongly affected by our off-centre ion is the 3s state. Such a state will not be greatly affected by the high-order icosahedral symmetry.

3. Magnesium ion pseudopotential

In contrast to earlier works [12–14], which only use the bare charge potential to describe the ions, we describe the conduction electrons' interaction with the Mg^{++} closed shell core by a local pseudo-potential of the form (in au)

$$V_{ext}(r) = -\frac{2}{r} + a\frac{\exp(-kr)}{r} \tag{7}$$

with $a = 20.657$ and $k = 2.5501$. At large r, the electrons see the net charge of the Mg^{++}. Closer in, more of the nuclear charge of the ion is unscreened by its close-shell core electrons. The resulting low-lying spectrum for Mg^+ is compared with the experimental spectrum in table 1. With the exception of states 3d and 3f, this

Table 1. The computed spectrum of Mg^+ using our pseudopotential. The energies are in eV. The experimental values are converted from cm^{-1} to eV from [22].

Config.	3s	4s	5s	6s	3p	4p	5p	6p	3d	4d	5d	4f	5f
Cal.	−15.03	−6.46	−3.57	−2.26	−10.50	−5.01	−2.94	−1.93	−5.91	−3.33	−2.13	−3.40	−2.17
Expt.	−15.03	−6.38	−3.53	−2.24	−10.60	−5.04	−2.95	−1.94	−6.17	−3.46	−2.21	−3.40	−2.18

pseudo-potential gives a fairly accurate representation of the low-lying spectrum of Mg^{+} and is superior to just the bare charge description.

4. Computational approach

To examine the delocalization of the magnesium ion, we must solve the Kohn–Sham equation in an axially symmetric geometry. The Mg^{++} ion is assumed to be located on the z axis. The most straightforward approach is to solve the KS equation directly in cylindrical coordinates. In this geometry, the single particle wavefunctions are of the form

$$\psi_{\mathbf{i}}(\mathbf{r}) = r^{1/2} u_{m,n}(r, z) \exp(\mathrm{i}m\phi), \tag{8}$$

with the radial functions $u_{m,n}(r, z)$ determined by the 2D KS equation

$$\frac{\hbar^2}{2\mu}\left[-\frac{\mathrm{d}^2}{\mathrm{d}z^2} - \frac{\mathrm{d}^2}{\mathrm{d}r^2} + \frac{4m-1}{4r^2}\right] u_{mn,}(r, z) + V_{\mathrm{H}}(r, z) u_{m,n}(r, z) = \varepsilon_{m,n} u_{m,n}(r, z). \tag{9}$$

Here, $\mathbf{i} = \{n, m\}$ denotes the pair of principal and azimuthal quantum numbers n and m, and μ is the reduced mass. We solved equation (9) by discretizing the derivative operators and applied standard matrix eigenvalue methods. Some care must be exercised in the discretization of the second derivative in the radial direction to take care of the non-analytic character of the radial functions. Solving the two-dimensional Schrödinger equation for the lowest few states is then non-trivial, but still feasible with conventional numerical methods. To obtain an initial approximation for the eigenstates, we first solve the eigenvalue equation on a coarse mesh, using conventional LAPACK routines. We then improve the solution by inverse iterations on a mesh with grid size of 0.1 au, with 180 mesh points in each r and z direction.

The second part of the problem is the self-consistent determination of the effective potential $V_H(\mathbf{r})$. For that purpose, we have used a recently developed [18] algorithm that displays robust convergence properties.

As a consistency test, we have independently solved the KS equation in the spherically symmetric cases for the undoped fullerenes and cases where the Mg^{++} ion is fixed at the centre of the fullerene. The simpler spherical geometry allows for a more accurate numerical treatment, not just because larger meshes and finer discretizations are possible with an effectively one-dimensional calculation, but also because spherical coordinates match the physical geometry better. The agreement between the two calculations is typically at the percent level. For example, we obtain, for the neutral, undoped cluster in the spherically symmetric calculation a correlation energy of -8.88 eV per particle, and in the cylindrical symmetry -8.91 eV.

5. Results

5.1. *Structure*

We will first determine the equilibrium location of the magnesium ion. Figure 2 shows the difference between the ground state energy in LDA for the endohedral system as a function of the displacement coordinate z of the Mg^{++} ion from the fullerene's centre. The net charge of the $Mg@C_{60}$ complex is $+1$, 0 and -1,

respectively, corresponding to a total electron number $N = 241$, 242 and 243. We wanted to see whether adding or removing an electron will significantly change the charge distribution of the system. Within the framework of our stated calculation, for all three charge configurations, we observed a shallow energy minimum of about 0.6 eV when the Mg^{++} ion is displaced 2 au off the centre. This small energy difference is about one part in 10^4 of the total energy of the system. While DFT cannot claim absolute energy accuracy on this scale, we believe that since we are computing energy difference between two locations, this relative energy difference can be reliable. The calculation suggests that the Mg^{++} ion will be easily delocalized from the fullerene's centre. Figure 2 also shows that there is very little change of the energetics as a function of the total charge—which indicates that the Mg ion inside the fullerene cage remains fully ionized.

Figure 3 show surface plots of the electron density of the compound system as a function of the magnesium ion delocalization. As it is intuitively evident, since the fullerene is hollow, a small displacement of the ion from the centre has little effect on the electron shell density; at $z = 3.0$ au we only see a small wrinkle in the electron density. Only when the Mg^{++} ion is within the fullerene shell do we see a noticeable change in the electron density. (This is of course, an energetically unfavourable configuration.) In all cases where the ion is at the centre, charged and uncharged, we found no significant electron density in the vicinity of the Mg^{++} ion, suggesting that the Mg ion inside the fullerene cage remains doubly ionized. (See our above comment in connection with figure 2.)

To gain some insights into various situations, we show for the spherically symmetric case, the resulting self-consistent potential $V_H(r)$, equation (2), for both undoped and doped, neutral and charged systems in figure 4. One observes that a global charge change of the system produces only an up- or down-shift of the shell potential. Near the centre, the Mg^{++} ion is far from the C_{60} cage and has little effect on this self-consistent electronic potential.

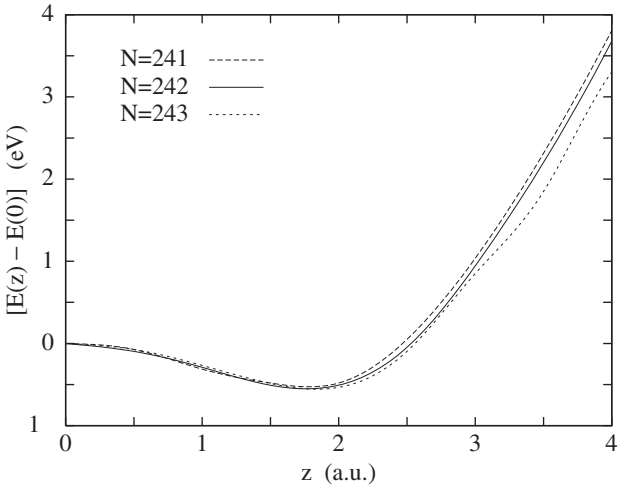

Figure 2. The energy difference between the displaced and centred Mg^{++} ion as a function of the off-centre displacement z, for singly positive ($N = 241$), neutral ($N = 242$) and singly negative charged ($N = 243$) endohedral systems. The energy minimum is about 0.6 eV below the on-centre energy at $z = 0$.

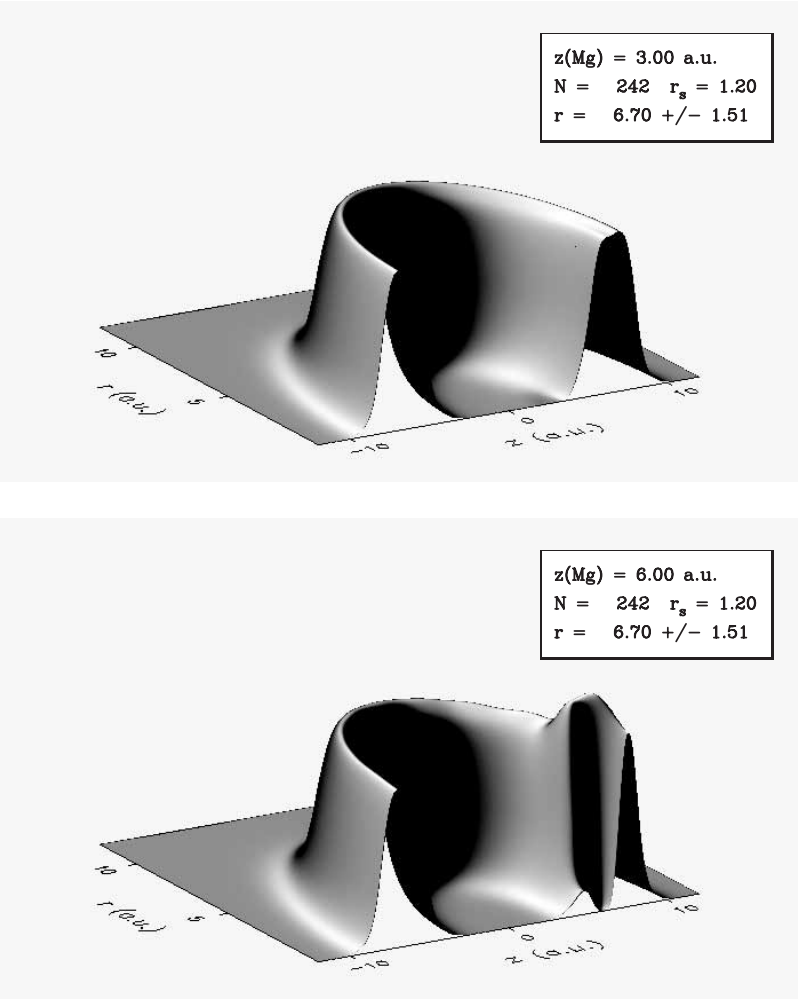

Figure 3. The electron density of a neutral endohedral fullerene with the Mg^{++} ion $z = 3$ au (upper figure) and at $z = 6$ au (lower figure). The effect of the Mg ion is only a minute ripple even at $z = 3$ au.

5.2. *Single particle energies*

Figure 5 shows the single-particle energies of bound states for both the doped and the undoped fullerenes. These spectra are labelled as in calculations with cylindrically symmetric geometry, i.e. the states are characterized by a principle quantum number n and an azimuthal quantum number m. Including the spin-degeneracy, states for $m = 0$ are doubly occupied whereas states for $m \neq 0$ have quadruple occupation. Since the geometry is in fact spherical, the degeneracy is actually higher; from the multiplicity of each eigenvalue one can read off the orbital angular momentum for each state. For very high lying states, the degeneracy for different values of m is not exact; this is just a numerical artefact coming from the cylindrical discretization box. Of course, one can verify the accuracy of the calculation by comparing with an independent solution of the KS equation in spherical geometry.

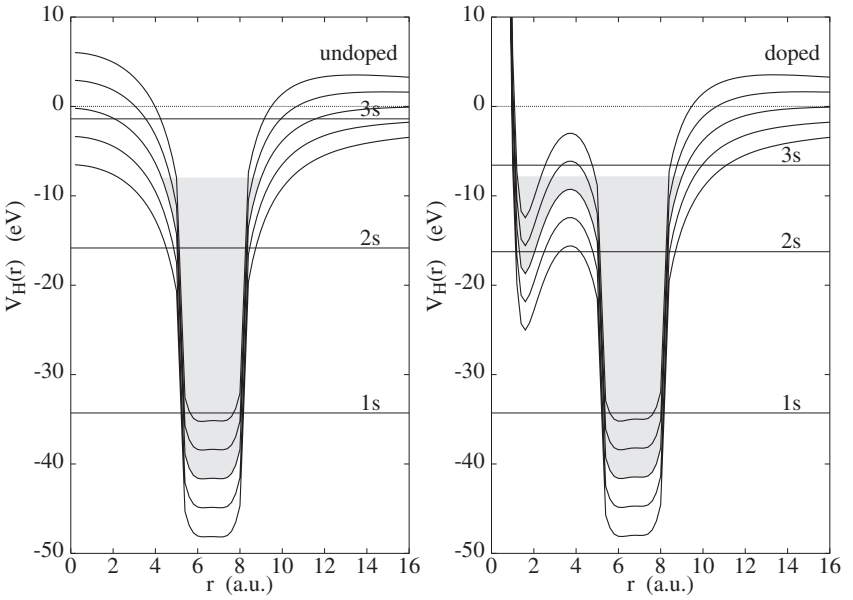

Figure 4. The self-consistent potential $V_H(r)$ for the undoped (left figure) and doped (right figure) fullerenes with total charge +2, +1, 0, −1 and −2 (from top to bottom). Clearly visible in the right figure is the repulsive core and the attractive well of the Mg^{++} pseudopotential. The grey-shaded areas are the regimes between $V_H(r)$ and the Fermi energy of the (undoped or doped) endohedral complex. The three heavy horizontal lines are the energies of the 1s, 2s and 3s electrons in this system. Only the 3s state is significantly affected by the introduction of the Mg ion.

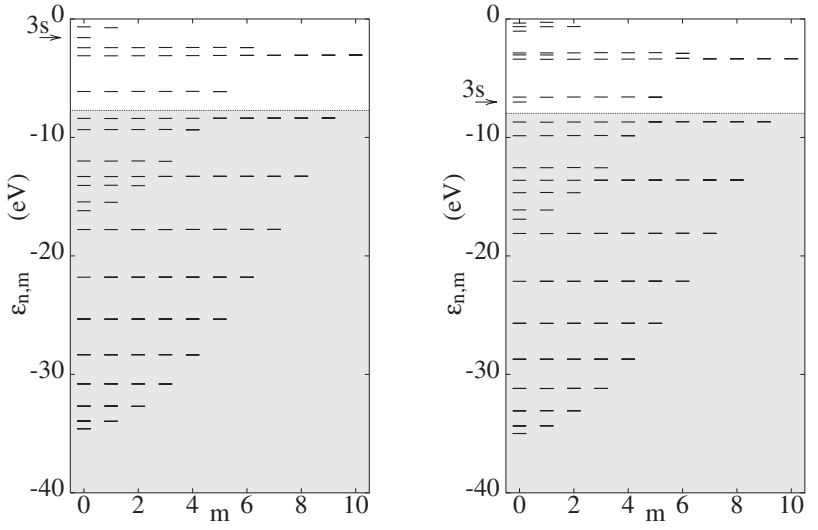

Figure 5. The bound state single-particle spectrum $\varepsilon_{n,m}$ for an undoped fullerene (left figure) and for a fullerene doped with a Mg^{++} impurity at the centre (right figure). Note the degeneracy of the states for different azimuthal quantum number m. Note also the shift of the 3s state (pointed to by arrows) between the doped and the undoped case. The grey-shaded area identifies the occupied states.

The two spectra are almost identical, particularly for the *occupied* orbitals, which lie in the grey-shaded areas in figure 5. The most interesting feature of the doped fullerene is the proximity of the 3s state to the Fermi energy. By doping the fullerene, the 3s state is lowered from −1.5 to −7.36 eV. There is also a visible shift in the 3p state from −0.67 to −3.0 eV, but these states are already very loosely bound. The identification of these states as s states stems, in cylindrical geometry, from the degeneracy as seen in figure 5. Figure 6 shows the wavefunctions for the 1s, 2s and 3s state on both the undoped and the doped system. Evidently, the 1s wave functions are almost identical, and the 2s wave functions remain very similar in both cases. The 3s wave functions differ significantly for a very understandable reason. Whereas this state describes, in the *undoped* system, an electron that is free to move through out the cage, in the doped case, it is mostly bound to the Mg^{++} ion. The additional binding is evidently due to the attractive portion of the Mg^{++} pseudopotential.

Since the lowering of the 3s state is the most pronounced feature of doping, it is interesting to see how this state changes relative to the other states as a function of the off-centre displacement of the Mg^{++} ion. Figure 7 shows the development of the individual states as a function of the Mg^{++} location. As the Mg^{++} ion moves off-centre, the degeneracy of the $L = 5$ state close to the 3s state is broken, but this degeneracy breaking is quite small compared to the shift of the 3s state.

The reason behind this is that when the ion moves off-centre, it must drag the 3s wave function off-centre with it. Since the 3s electron is repelled by electrons in the shell, it will be squeezed between the ion and the fullerene shell and its kinetic energy goes up. Only a wavefunction that is strongly dragged by the ion will be affected; this explains why only the 3s state is shifted significantly. Finally, when

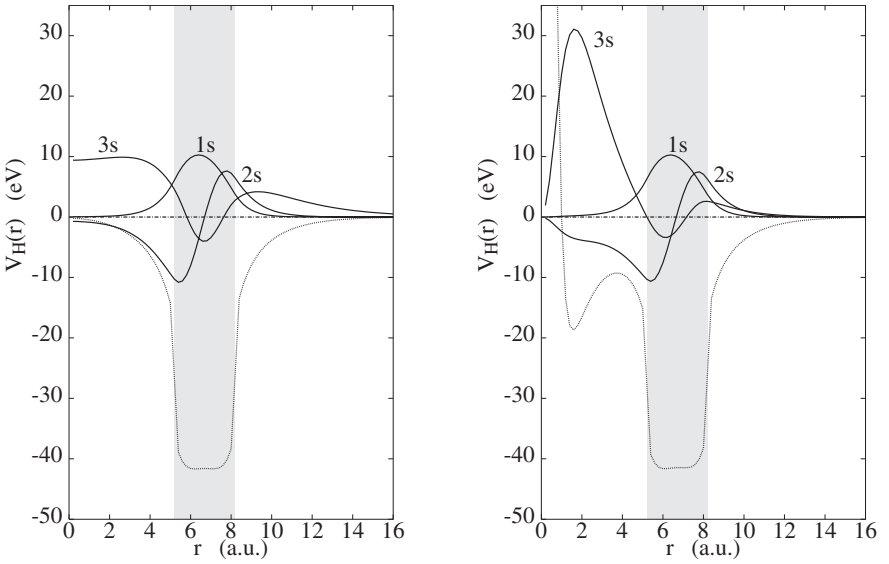

Figure 6. The 1s, 2s and 3s wave function for an undoped fullerene (left figure, solid lines, arbitrary scale) and for a fullerene doped with a Mg^{++} impurity at the centre (right figure, solid lines, arbitrary scale). Also shown for comparison is the self-consistent potential $V_H(r)$ (dashed lines, left scale). The grey-shaded areas indicates the range of the jellium background.

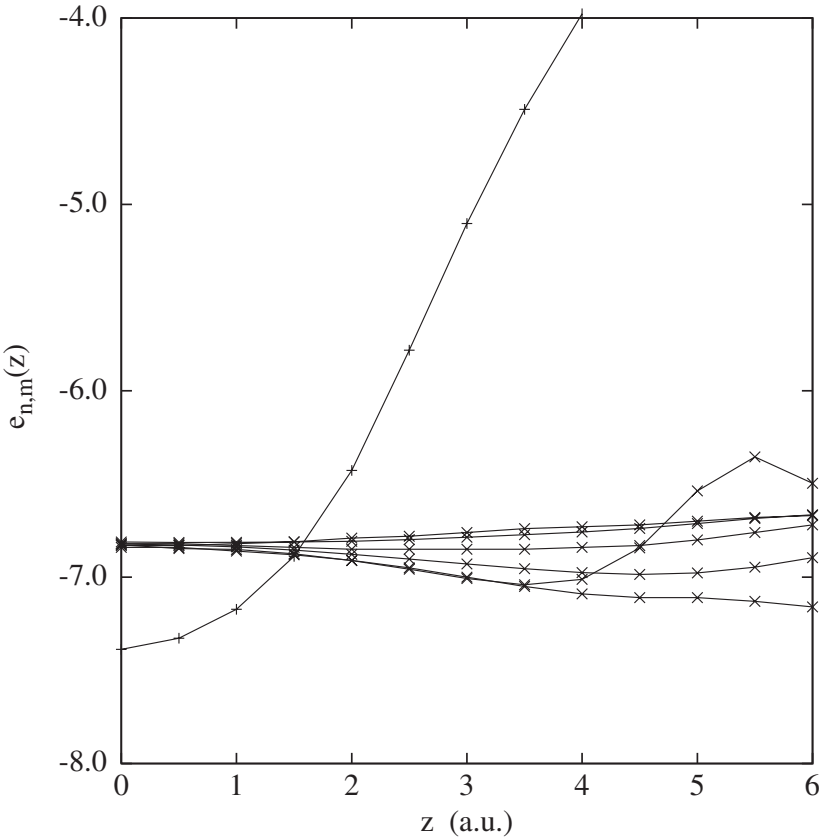

Figure 7. The change in the energy of the 3s state (solid line with + markers) as well as the $\ell = 5$ states (dashed lines with × markers) as a function of the displacement z of the Mg^{++} ion from the centre of the fullerene cage. The lifting of degeneracy as the ion moves off-centre is clearly visible.

the Mg^{++} approaches the fullerene shell, the weakly bound electron begins to feel the Pauli exclusion of the other electrons, and is 'squeezed' off the Mg^{++} ion.

5.3. *Polarizability and photoabsorption cross-section*

The excitations of the endohedral system can be directly observed in the photoabsorption cross section. To calculate the latter, we apply the standard method of time-dependent density functional theory [19, 23, 24]. The photoabsorption cross-section $\sigma(\omega)$ is obtained from the frequency-dependent, complex polarizability $\alpha(\omega)$ through

$$\sigma(\omega) = 4\pi \frac{\omega}{c} \Im m\alpha(\omega), \tag{10}$$

where [24]

$$\alpha(\omega) = -e^2 \int \mathrm{d}^3 r \, \mathrm{d}^3 r' z \chi(\mathbf{r}, \mathbf{r}'; \omega) z' \tag{11}$$

and $\chi(\mathbf{r},\mathbf{r}';\omega)$ is the density–density response function. In the random-phase approximation, the response function is determined by the intergal equation

$$\chi(\mathbf{r},\mathbf{r}';\omega) - \int \mathrm{d}^3 r_1\, \mathrm{d}^3 r_2 \chi_0(\mathbf{r},\mathbf{r}_1;\omega) V_{\mathrm{p-h}}(\mathbf{r}_1,\mathbf{r}_2)\chi(\mathbf{r}_2,\mathbf{r}';\omega) = \chi_0(\mathbf{r},\mathbf{r}';\omega), \tag{12}$$

where $\chi_0(\mathbf{r},\mathbf{r}';\omega)$ is the density–density response function of non-interacting electrons in the potential $V_{\mathrm{H}}(\mathbf{r})$ given by [25]

$$\chi_0(\mathbf{r},\mathbf{r}';\omega) = \sum_{\mathrm{ph}} \psi_{\mathrm{p}}(\mathbf{r})\psi_{\mathrm{h}}^*(\mathbf{r})\left[\frac{1}{\hbar\omega - \varepsilon_{\mathrm{p}} + \varepsilon_{\mathrm{h}} + \mathrm{i}\eta} - \frac{1}{\hbar\omega + \varepsilon_{\mathrm{p}} - \varepsilon_{\mathrm{h}} - \mathrm{i}\eta}\right]\psi_{\mathrm{p}}^*(\mathbf{r}')\psi_{\mathrm{h}}(\mathbf{r}'). \tag{13}$$

Here, we label the *occupied* ('hole') states as 'h' and the *unoccupied* ('particle') states as 'p'. $V_{\mathrm{p-h}}(\mathbf{r},\mathbf{r}')$ is the 'particle–hole interaction'. In the simple local density approximation it is just the bare Coulomb potential *plus* a contact interaction,

$$V_{\mathrm{p-h}}(\mathbf{r},\mathbf{r}') = \frac{e^2}{|\mathbf{r}-\mathbf{r}'|} + \left.\frac{\mathrm{d}v_{xc}[\rho]}{\mathrm{d}\rho}\right|_{\rho=\rho(r)} \delta(\mathbf{r}-\mathbf{r}'). \tag{14}$$

We begin our calculations of the density–density response function with the spherically symmetric case. In this case, we can expand the density–density response function in spherical harmonics

$$\chi(\mathbf{r},\mathbf{r}';\omega) = \sum_{\ell,m} \chi_\ell(r,r';\omega) Y_{\ell m}(\hat{\mathbf{r}}) Y_{\ell m}^*(\hat{\mathbf{r}}') \tag{15}$$

and obtain

$$\alpha(\omega) = -\frac{4\pi}{3} e^2 \int \mathrm{d}r\, \mathrm{d}r' r^3 r'^3\, \chi_1(r,r',;\omega). \tag{16}$$

Although equation (13) sums over all particle states, it is well known that the free density–density response function can be calculated from the occupied states alone *plus* a Green's function [23, 24]. In this work, we have directly summed over particle states using equation (13). The continuum states can be simply generated by solving the KS equation in a huge box, with a finite imaginary part δ in the frequency which is comparable to the level spacing in that box. A radius of $1000\,a_0$ is sufficient, but even going to $4000\,a_0$ is not a computational problem, yielding an energy resolution of 0.02 eV. The advantage of this procedure is that the first two sum rules for $\chi_0(\mathbf{r},\mathbf{r}';\omega)$ are exactly satisfied for *any* discretization, as a consequence of the completeness and closure relation of the solutions of the discretized Kohn–Sham equation; it is also easily implementable and tested.

For photoabsorption, the frequency interval of interest is between 0 and 10 eV. This is because a prime signature of the endohedral magnesium ion is the transition from the 3s state at -7.36 eV to the 2p state at -16.35 eV, with an energy difference of 8.99 eV. This transition is in the continuum, with energies above the chemical potential, but it is still a discrete state because the channel continuum for the s–p state transition starts at $16.35\,\mathrm{eV} + e_{\mathrm{F}} \approx 32.3$ eV, i.e. it will be seen as a discrete excitation within a contimuum.

The only other two low-energy transitions are one from $(n=2,\ell=5)$ to $(n=1,\ell=4)$ at $\Delta E = 3.2$ eV and from $(n=1,\ell=10)$ to $(n=1,\ell=9)$ at $\Delta E = 5.3$ eV. These transitions are between electronic states of the fullerene cage

and are very similar whether or not there is an entrapped atom. We therefore restrict our discussion only to the interval between 8 and 10 eV, the results in other energy regimes are expected and found to be similar to those of [19].

Figure 8 shows the imaginary part of the frequency-dependent polarizability $\alpha(\omega)$ for both doped and undoped fullerenes in the energy regime from 8.0 to 10 eV. The doped fullerene displays a peak at an energy of 8.8 eV, which compares well with the energy of the transition from the 3s to the 2p state. No such peak is seen in the undoped case.

It is very fortunate that in our system, only one state, the 3s state, is strongly coupled to the magnesium ion. Thus, as the ion moves off-centre only the energy of the 3s state is significantly raised. Therefore even without directly computing the off-centre dynamic polarizability, one can infer that the resonance peak initially at 8.8 eV will simply move higher in energy. According to figure 2, the ion can easily move off-center by $\approx$3 au, causing the 3s state to rise and the resonance peak to shift by $\approx$2 eV (see figure 7). The resonance peak will be accompanied by side bands [13] due to the vibrational motion of the ion about its minimum. This detail is not considered here.

6. Summary

In this work, we have computed the off-centre dyanmics and optical response of an endohedral fullerene complex containing a Mg ion. The key findings of our work are that: (1) the energetically favoured location of the Mg^{++} is off centre, by about 1 Å. This is an important piece of structural information. This delocalization effect reduces the system's symmetry from spherical to cylindrical and results in a general splitting of any $(2L+1)$-fold degenerate state into $L+1$ distinct levels. This is illustrated for the case of $L=5$ in figure 7. The magnitude of these splittings is generally small; we have not considered in any detail their experimental consequences. (2) Only one state, the 3s state, is significantly raised in

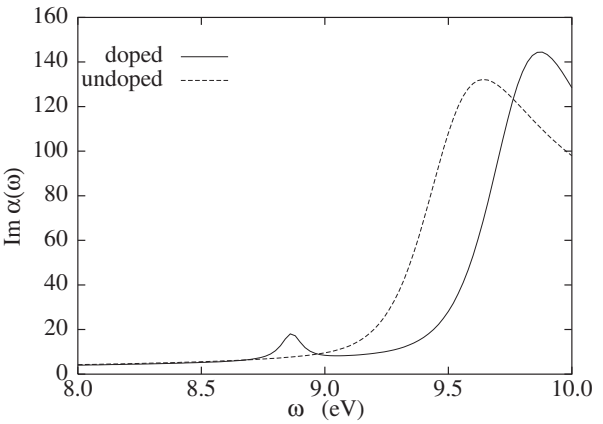

Figure 8. The imaginary part of the frequency-dependent polarizability $\alpha(\omega)$. The doped fullerene (solid line) displays a pronounced peak at an energy of 8.8 eV, which compares well with the energy of the transition from the 3s to the 2p state. No such peak is seen in the undoped case (dashed lines). For clarity, we do not show other transition peaks which are similar and common to both the doped and undoped case.

energy by the presence of the Mg ion. By computing the imaginary part of the dynamic polarizability, we show that this results in a resonance peak which corresponds to the 2p–3s transition at 8.8 eV or 140 nm. This peak is not present for undoped fullerenes. (3) As the Mg^{++} ion is displaced off-centre, the 3s state will rise in energy and produce an absorption peak shifting toward higher energy. Thus in our calculation this resonance peak tracks the location of the Mg^{++} ion. It is of great experimental interest to see whether this can be observed.

At present the multiphoton ionization of exohedral MgC_{60}^{+} using continuous--wave (cw) single mode lasers has been measured [7]. Since ionization is a multi-photon process with an order determined by the number of photons required by the ionization potential, experimentally, one expects to observe a narrow two-photon peak and a broad multi-photon feature. In addition after absorption and excitation, also fragmentation by emission of C_2 molecules, and delayed metastable fragmentation indicative of high excitations of the parent endohedral complex should occur. We plan to extend these studies to endohedral $Mg@C_{60}^{+}$ so that the detailed scenario of optical response suggested by the present calculation can be tested.

It is well known, and documented in the work of [19], that the jellium model misses a number of the finer details of the C_{60} structure. We believe that the generic effect that we are describing is not affected by these shortcomings of the jellium model: our main conclusion is that there is a low-lying dipole resonance between the 2p orbital and the fullerene and the 3s orbital which is, in the doped case, a state where the electron is bound to the endohedral Mg ion (an experimentally known quantity) and whose energy is close to the Fermi energy of the fullerene (whose energy is also experimentally known). Both, the 3s and the 2p state are states of high angular symmetry which should be only weakly affected by the high multipole icosahedral structure of the discrete ions. Our prediction is that the energy of this resonance should go *up* as the Mg ion is displaced from the centre location.

Our work should stimulate further examination of the effect in more sophisticated models. A full coordinate-space calculation along the line of Yabana and Bertsch [26] would be a welcome improvement. However, it should be noted that that work uses a mesh of only 42 691 points at a grid size of 0.6 au. Such a grid size is insufficient for an accurate numerical treatment of the effect described here; this can be inferred simply from looking at the Mg^{++} pseudopotential and the steep electron density shown in figure 4 (*a*). Our experience suggests that a reliable calculation would at least require a grid size of $\approx$0.1 au with 128^3 mesh points. This would need 2 Gigabyte of memory just to store the 120 wave functions and correspondingly, significant additional computational resources. Until such a calculation has been completed, our simplified calculation, based on the jellium model, which predicted the effect, is justified and appropriate.

Acknowledgments

This work was supported, in part, by the Austrian Science Fund under project P-15083 (to EK), by the National Science Foundation under grant No. PHY-0100839 (to SAC), the Texas Advanced Research Program under proposal number 010366-082 (to HAS and SAC), and the Robert A. Welch Foundation under grant number A-2546 (to HAS).

References

[1] Shinohara, H., 2000, *Rep. Prog. Phys.*, **63,** 843.
[2] Liu, S., and Sun, S., 2000, *J. Organometallic Chem.*, **599,** 74.
[3] Shinohara, H., *et al.*, 1995, *J. Phys. Chem.*, **99,** 13769.
[4] Welling, M., Schuessler, H. A., Thompson, R. I., and Walther, H., 1997, *Int. J. Mass Spectrom. Ion Proc.*, **172,** 95.
[5] Dietrich, F., and Walther, H., 1987, *Phys. Rev. Lett.*, **58,** 203.
[6] Birkl, G., Kassner, S., and Walther, H., 1992, *Nature*, **357,** 310.
[7] Thompson, R. I., Welling, M., Schuessler, H. A., and Walther, H., 2002, *J. Chem. Phys.*, **116,** 10201.
[8] Weiss, F. D., *et al.*, 1988, *J. Am. Chem. Soc.*, **110,** 204.
[9] Suzuki, S., *et al.*, 1997, *Z. Phys.* D, **40,** 410.
[10] Rohmund, F., *et al.*, 2000, *Chem. Phys. Lett.*, **323,** 173.
[11] Cioslowski, J., 1995, *Electronic Structure Calculations on Fullerenes and Their Derivatives* (New York, Oxford: Oxford University Press).
[12] Cioslowski, J., and Fleischmann, E. D., 1991, *J. Chem. Phys.*, **94,** 3730.
[13] Ballester, J. L., and Dunlap, B. I., 1992, *Phys. Rev.* A, **45,** 7985.
[14] Schmidt, P. P., Dunlap, B. I., and White, C. T., 1991, *J. Chem. Phys.*, **95,** 10537.
[15] Dreizler, R., and Gross, E., 1990, *Density Functional Theory* (Berlin, New York: Springer Verlag).
[16] Kohn, W., and Vashishta, P., 1983, *Theory of the Inhomogeneous Electron Gas,* edited by S. Lundqvist and N. H. March (New York: Plemum), p. 79.
[17] Van Orden, A., and Saykally, R. J., 1998, *Chem. Rev.*, **98,** 2313.
[18] Auer, J., and Krotscheck, E., 1999, *Comput. Phys. Commun.*, **118,** 139.
[19] Puska, M. J., and Nieminen, R. M., 1993, *Phys. Rev.* A, **47,** 1181.
[20] Ren, S. L., *et al.*, 1991, *Appl. Phys. Lett.*, **59,** 2678.
[21] Saito, R., Dresselhaus, G., and Dresselhaus, M. S., 1992, *Phys. Rev.* B, **46,** 9906.
[22] Moore, C. E., 1949, *Atomic Energy Levels*, Vol. I. (United States Department of Commerce, National Bureau of Standards).
[23] Stott, M. J., and Zaremba, E., 1980, *Phys. Rev.* A, **21,** 12.
[24] Zangwill, A., and Soven, P., 1980, *Phys. Rev.* A, **21,** 1561.
[25] Fetter, A. L., and Walecka, J. D., 1971, *Quantum Theory of Many-Particle Systems* (New York: McGraw-Hill).
[26] Yabana, K., and Bertsch, G. F., 1996, *Phys. Rev.* B, **54,** 4494.